Chimica Techno Acta
published by Ural Federal University
eISSN 2411-1414
chimicatechnoacta.ru

ARTICLE
2023, vol. 10(2), No. 202310211
DOI: 10.15826/chimtech.2023.10.2.11

Synthesis and cytotoxic activity of (2-arylquinazolin-4-yl)hydrazones of 2-hydroxybenzaldehydes

Emiliya V. Nosova [ab*], Ilya I. Butorin [a], Margarita D. Likhacheva [a], Svetlana K. Kotovskaya [a]

a: Institute of Chemical Engineering, Ural Federal University, Ekaterinburg 620009, Russia
b: I. Postovsky Institute of Organic Synthesis, Ural Division of the Russian Academy of Sciences, Ekaterinburg 620219, Russia
***** Corresponding author: emilia.nosova@yandex.ru

This paper belongs to a Regular Issue.

Abstract

2-Phenyl-6,7-difluoro and 2-(4-fluorophenyl)quinazoline derivatives bearing salicylidenhydrazino fragments at position 4 were prepared based on 4,5-difluoroantranilic acid or anthranilamide. Molecular docking to casein kinase 2 was performed; compounds with high *in silico* activity to CK2 were revealed. Cytotoxic activity of the synthesized compounds was studied on cancer cell line MDA-MB-231 and normal cell line WI26 VA4.

Keywords

2-arylquinazolines
salicylidenhydrazines
in silico activity
casein kinase 2 inhibitor
cytotoxic activity

Received: 28.03.23
Revised: 26.04.23
Accepted: 27.04.23
Available online: 04.05.23

Key findings

- N-Salicylidene-N'-(6,7-difluoro-2-phenylquinazolin-4-yl)-hydrazines were obtained based on 4,5-difluoroantranilic acid.
- N-Salicylidene-N'-(2-(4-fluorophenyl)quunazolin-4-yl)-hydrazines were synthesized based on anthranilamide.
- Molecular docking towards casein kinase 2 was performed, cytotoxic activity was studied.

Supplementary materials

1. Introduction

Fluorine-containing quinazoline derivatives represent a class of anticancer agents. Phosphoinositide 3-kinase and Idelalisib (Zydelig) is used as a medication to treat certain blood cancers; the molecule acts as inhibitor of P110δ, the delta isoform of the enzyme phosphoinositide 3-kinase [1]. Gefitinib (Iressa) is a selective EGFR tyrosine kinase (EGFR-TK) inhibitor. This agent retards growth of various human tumor cell lines, metastasis, and angiogenesis, accelerates the apoptosis of tumor cells and enhances the efficiency of chemotherapy, radiation, and hormone therapy [2]. Casein kinase 2 is a promising template for designing anticancer drugs. Protein kinase CK2 is a ubiquitous, highly conserved, and constitutively active serine/threonine protein kinase; overexpression and hyperactivation of CK2 was observed in a wide variety of cancers, including breast, lung, prostate, colorectal, and renal [3–11]. For this reason, CK2 represents an attractive target for chemotherapy [12–16]. Anilino-substituted 2,6-naphthyridines were found to act as potent CK2 protein kinase inhibitors [17]. The search of antitumor agents inhibiting kinases among bi- and tricyclic derivatives of six-membered heterocycles with two nitrogen atoms is promising [18–23].

(2-Phenylquinazolin-4-yl)hydrazones of 2-hydroxybenzaldehydes **1a–c**, **2a–c**, **3a**,**b** (Figure 1) were reported previously [24].

The aim of the present article is to describe a series of new 2-arylquinazolines **3c**,**d**, **9a**,**b**, bearing salicylidenhydrazino group at position 4, to estimate the interaction of quinazolines **1–3**, **9** with important target of anticancer agents (CK2) by using molecular docking method, and to study cytotoxic and CK2 inhibition activity of some salicylidenhydrazino-substituted 2-arylquinazolines.

2. Experimental

2.1. General

Unless otherwise indicated, all common reagents and solvents were used from Sigma Aldrich without further purification.

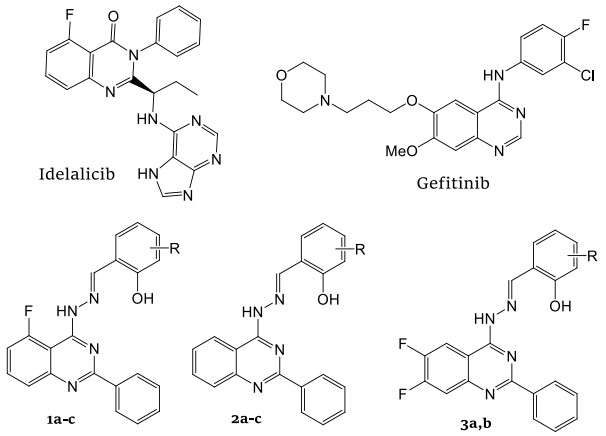

Figure 1 Structure of anticancer agents Idelalisib, Gefitinib and previously prepared salicilidenehydrazono substituted quinazolines (**1a–c, 2a–c, 3a,b**). **1, 2**: R = H (**a**), 4-OH (**b**), 3,5-diBr (**c**); **3**: R = H (**a**), 5-NO_2 (**b**).

The ^{1}H NMR, ^{13}C NMR and ^{19}F NMR spectra were obtained on a Bruker Avance II DMX400 spectrometer using DMSO-d_6 as the solvent. The ^{1}H NMR experiments chemical shifts were referenced to the hydrogen resonances of the solvent (DMSO, δ = 2.50 ppm). Carbon chemical shifts were referenced to the carbon resonances of the solvent ($CDCl_3$, δ = 77.16 ppm). ^{19}F NMR spectra were recorded with $CFCl_3$ (C_6F_6 was used as secondary reference, δ_F –162.9 ppm). Mass spectra were recorded on a SHIMADZU GCMS-QP2010 Ultra instrument with electron ionization (EI) of the sample. Microanalyses (C, H, N) were performed using a Perkin–Elmer 2400 elemental analyzer. Melting points were measured on the instrument Boetius. Microanalyses (C, H, N) were performed using the Perkin–Elmer 2400 elemental analyzer.

2.2. Preparation of intermediates

2.2.1. (*E*)-2-(4-Fluorophenylydeneamino)benzamide (6)

4-Fluorobenzaldehyde (0.67 g, 5.4 mmol) was added to a solution of 2-aminobenzamide **5** (0.74 g, 5.4 mmol) in ethanol (9.62 mL). The mixture was stirred at room temperature for 3 h, and the white precipitate was filtered off and recrystallized from acetonitrile. Yield 1.07 g (82 %), mp 194–196 °C (lit. 197–200 °C [25]). ^{1}H NMR, δ, ppm: 7.18 *d* (1H, Ar, ^{3}J 8.1 Hz), 7.25–7.40 *m* (3H, Ar), 7.4 *br. s* (1H, NH), 7.5–7.6 *m* (2H, Ar), 7.95–8.05 *m* (2H, Ar), 8.2 *br. s* (1H, NH), 8.59 *s* (1H, CH=N). ^{19}F{H} NMR, δ, ppm: –107.05 s. Found, %: C 69.32, H 4.62, N 11.49. $C_{14}H_{11}FN_2O$. Calculated, %: C 69.41, H 4.58, N 11.56.

2.2.2. 2-(4-Fluorophenyl)quinazolin-4(3*H*)-one (7)

Copper(II) chloride (0.67 g, 4.9 mmol) was added to the suspension of 2-(4-fluorophenylydeneamino)benzamide **6** (0.90 g, 3.7 mmol) in ethanol (14 mL) and the mixture was refluxed for 5 h. After cooling the precipitate was filtered off and recrystallized from dimethyl sulfoxide. Yield 0.705 g (79%), mp 282–284 °C (lit. 284–286 °C [36]). ^{1}H NMR, δ, ppm: 7.26–7.31 m (2H, Ar), 7.46–7.49 *m* (1H, Ar), 7.68–7.70 *m* (1H, Ar), 7.77–7.81 *m* (1H, Ar), 8.13–8.15 m (1H, Ar), 8.27–8.30 *m* (2H, Ar), 12.4 *br. s* (1H, NH). ^{19}F{H} NMR, δ, ppm: –108.90 s. Found, %: C 70.11, H 3.90, N 11.53. $C_{14}H_9FN_2O$. Calculated, %: C 69.99, H 3.78, N 11.66.

2.2.3. 2-(4-Fluorophenyl)-4-chloroquinazoline (8)

Phosphorus oxychloride (3.2 mL) was added to quinazolin-4-one **7** (0.65 g, 2.7 mmol), and the mixture was refluxed for 2 h. The reaction mixture was cooled to room temperature and poured onto ice. The white precipitate was filtered off, washed with water, dried in air and used without additional purification. Yield 0.52 g (75%), mp 148–150 °C. ^{1}H NMR, δ, ppm: 7.41–7.45 *m* (2H, Ar), 7.86–7.88 *m* (1H, Ar), 8.14–8.15 *m* (2H, Ar), 8.29–8.32 *m* (1H, Ar), 8.53–8.57 *m* (2H, Ar). ^{19}F{H} NMR, δ, ppm: –109.38 s. Found (%): C 64.89, H 3.03, N 10.92. $C_{14}H_8ClFN_2$. Calculated (%): C 65.00, H 3.12, N 10.83.

2.2.4. 2-(4-Fluorophenyl)-4-hydrazinoquinazoline (4b)

Hydrazine monohydrate (0.72 mL, 9.7 mmol, 65% solution) was added to a solution of 4-chloroquinazoline **8** (0.5 g, 1.94 mmol) in ethanol (10 mL). The mixture was stirred at 70 °C for 3 h, then cooled. The bright yellow precipitate was filtered off and recrystallized from acetonitrile. Yield 0.39 g (80%), mp 174–176 °C. ^{1}H NMR, δ, ppm: 4.8 *br. s* (2H, NH2), 7.19–7.24 *m* (2H, Ar), 7.35–7.45 *m* (1H, Ar), 7.65–7.72 *m* (2H, Ar), 8.15–8.20 *m* (1H, Ar), 8.60–8.63 *m* (2H, Ar), 9.6 *br. s* (1H, NH). ^{19}F{H} NMR, δ, ppm: –111.81 s. Found (%): C 66.04, H 4.27, N 22.12. $C_{14}H_{11}FN_4$. Calculated (%): C 66.13, H 4.36, N 22.03.

2.3. Preparation of target hydrazonoquinazolines 3c, d, 9a, b

General method. The corresponding salicylic aldehyde (0.897 mmol) was added to a solution of 4-hydrazinoquinazoline **4a** or **4b** (0.753 mmol) in ethanol (7 mL). The reaction mixture was refluxed for 1.5 h, then cooled; the precipitate formed was filtered off and recrystallized from ethanol.

2.3.1. *N*-(3,5-Di(*t*-butyl)salicylidene)-*N*'-(6,7-difluoro-2-phenylquinazolin-4-yl)-hydrazine (3c)

Yield 83%, mp 184–186 °C. NMR, δ, ppm: 1.37 s (9H, $3CH_3$), 1.55 *s* (9H, $3CH_3$), 7.25 *s* (1H, $H^{4''}$), 7.33 *s* (1H, $H^{6''}$), 7.49–7.53 *m* (3H, $H^{3'}$, $H^{4'}$, $H^{5'}$), 7.76 *dd* (1H, H^5, $^3J_{HF}$ 9.2, $^4J_{HF}$ 4.9 Hz), 8.42 *dd* (1H, H^8, $^3J_{HF}$ 9.2, $^4J_{HF}$ 4.9 Hz), 8.58 *s* (1H, CH=N), 8.68–8.72 *m* (2H, $H^{2'}$, $H^{6'}$), 12.0 *br. s* (1H, NH), 13.1 *br. s* (1H, OH). ^{19}F{H} NMR, δ, ppm: –136.94 *d* (1F, $^3J_{FF}$ 24.3 Hz), –128.62 *d* (1F, $^3J_{FF}$ 24.3 Hz). ^{13}C NMR: 29.32 ($3CH_3$), 31.34 ($3CH_3$), 33.89 (*s*, CMe_3), 34.76 (*s*, CMe_3), 108.87 (*s*, C-2''), 110.04 (*s*, C-3'', C-5''), 114.90 (*s*), 117.40 (*s*), 125.20 (*s*), 125.38 (*s*), 128.05 (*s*), 128.22 (*s*), 130.80 (*s*), 135.76 (*s*), 137.51 (*s*), 140.10 (*s*), 148.01 (*dd*, C-6 or C-7, $^1J_{CF}$ = 249.4, $^2J_{CF}$ = 12.6 Hz), 148.56 (*s*), 148.85 (*d*, C-5, C-8, $^2J_{CF}$ = 17.1 Hz), 153.60 (*dd*, C-7 or C-6, $^1J_{CF}$ = 254.9, $^2J_{CF}$ = 17.1 Hz), 155.11 (*s*), 155.61 (*s*), 159.85 (*s*). MS, *m/z* (I_{rel} (%)): 488 $[M]^+$ (99), 257 [M–di-*t*Bu-isobenzoxazole]$^+$ (100), 154 [M–di-*t*Bu-isobenzoxazole-PhCN]$^+$ (14). Found, %: C 71.41, H 6.32, N 11.39. $C_{29}H_{30}F_2N_4O$. Calculated, %: C 71.29, H 6.19, N 11.47.

 DOI: 10.15826/chimtech.2023.10.2.11

2.3.2. *N*-(5-Chlorosalicylidene)-*N'*-(6,7-difluoro-2-phenylquinazolin-4-yl)-hydrazine (3d)

Yield 78%, mp 192–194 °C. ^{1}H NMR, δ, ppm: 7.03 *d* (1H, H$^{3''}$, $^3J_{HH}$ 7.2 Hz), 7.28 *d* (1H, H$^{4''}$, $^3J_{HH}$ 7.2 Hz), 7.50–7.54 *m* (3H, H$^{3'}$, H$^{4'}$, H$^{5'}$), 7.63 *s* (1H, H$^{6''}$), 7.76 *dd* (1H, H^5, $^3J_{HF}$ 10.1, $^4J_{HF}$ 5.8 Hz), 8.50–8.52 *m* (1H, H^8), 8.57 *s* (1H, CH=N), 8.58–8.62 *m* (2H, H$^{2'}$, H$^{6'}$), 12.0–12.2 *br. s* (2H, NH, OH). ^{19}F{H} NMR, δ, ppm: –136.75 *d* (1F, $^3J_{FF}$ 24.0 Hz), –128.41 *d* (1F, $^3J_{FF}$ 24.0 Hz). ^{13}C NMR: 108.92 (*s*, C-2''), 114.72 (*s*), 114.85 (*s*), 118.41 (*s*), 120.40 (*s*), 122.87 (*s*), 127.86 (*s*), 128.44 (*s*), 130.54 (*s*), 130.74 (*s*), 137.52 (*s*), 143.57 (*s*), 146.97 (*s*), 149.08 (*s*), 149.23 (*d*, C-5, C-8, $^2J_{CF}$ = 17.1 Hz), 151.64 (*dd*, C-6 or C-7, $^1J_{CF}$ = 249.4, $^2J_{CF}$ = 12.6 Hz), 153.82 (*dd*, C-7 or C-6, $^1J_{CF}$ = 249.8, $^2J_{CF}$ = 16.5 Hz), 156.32 (*s*), 159.99 (*s*), 159.93 (*s*). MS, *m/z* (I_{rel} (%)): 410 [M]$^+$ (56), 257 [M–chloroisobenzoxazole]$^+$ (100), 154 [M–chloroisobenzoxazole-PhCN]$^+$ (29). Found, %: C 61.52, H 3.30, N 13.59. $C_{21}H_{13}ClF_2N_4O$. Calculated, %: C 61.40, H 3.19, N 13.64.

2.3.3. *N*-(3,5-Di(*t*-butyl)salicylidene)-*N'*-(2-(4-fluorophenyl)quinazolin-4-yl)-hydrazine (9a)

Yield 76%, mp 152–154 °C. ^{1}H NMR, δ, ppm: 1.36 *s* (9H, 3CH$_3$), 1.55 *s* (9H, 3CH$_3$), 7.20–7.24 *m* (3H, H$^{4''}$, H$^{3'}$, H$^{5'}$), 7.31 s (1H, H$^{6''}$), 7.59 *m* (1H, H^7), 7.85–7.89 *m* (2H, H$^{2'}$, H$^{6'}$), 8.34–8.36 *m* (1H, H^5), 8.62 *s* (1H, CH=N), 8.75–8.79 *m* (2H, H^6, H^8), 12.1 *br. s* (1H, NH), 13.3 *br. s* (1H, OH). ^{19}F{H} NMR, δ, ppm: –111.28 *s*. ^{13}C NMR: 29.33 (3CH$_3$), 31.34 (3CH$_3$), 33.89 (*s*, CMe$_3$), 34.76 (*s*, CMe$_3$), 112.14 (*s*, C-2''), 114.93, 115.14 (both s, C-3'', C-5''), 117.53 (*s*), 122.60 (*s*), 125.20 (*d*, C-3', C-5', $^2J_{CF}$ = 21.6 Hz), 126.09 (*s*), 127.98 (*s*), 130.34 (*d*, C-2', C-6', $^3J_{CF}$ = 8.8 Hz), 133.50 (*s*), 134.57 (*s*), 135.76 (*s*), 140.08 (*s*), 148.45 (*s*), 150.51 (*s*), 155.10 (*s*), 156.08 (*s*), 158.18 (*s*), 163.85 (*d*, C-4', $^1J_{CF}$ = 259.4 Hz). MS, *m/z* (I_{rel} (%)): 470 [M]$^+$ (67), 239 [M–di-*t*Bu-isobenzoxazole]$^+$ (100), 118 [M–di-*t*Bu-isobenzoxazole-FC$_6$H$_4$CN]$^+$ (12). Found, %: C 74.15, H 6.80, N 11.79. $C_{29}H_{31}FN_4O$. Calculated, %: C 74.02, H 6.64, N 11.91.

2.3.4. *N*-(5-Chlorosalicylidene)-*N'*-(2-(4-fluorophenyl)quinazolin-4-yl)-hydrazine (9b)

Yield 74%, mp 202–204 °C. ^{1}H NMR, δ, ppm: 7.02 *d* (1H, H$^{3''}$, $^3J_{HH}$ 7.1 Hz), 7.25–7.35 *m* (3H, H$^{4''}$, H$^{3'}$, H$^{5'}$), 7.58–7.62 *m* (2H, H$^{6''}$, H^7), 7.85–7.89 *m* (2H, H$^{2'}$, H$^{6'}$), 8.38–8.42 *m* (1H, H^5), 8.60–8.70 *m* (3H, CH=N, H^6, H^8), 12.2 *br. s* (1H, NH), 12.3 *br. s* (1H, OH). ^{19}F{H} NMR, δ, ppm: –111.13 *s*. ^{13}C NMR: 112.18 (*s*, C-2''), 115.20 (*s*), 115.48 (*s*), 118.28 (*s*), 118.48 (*s*), 120.30 (*s*), 122.78 (*s*), 126.11 (*s*), 127.87 (*d*, C-3', C-5', $^2J_{CF}$ = 21.7 Hz), 128.77 (*s*), 130.09 (*d*, C-2', C-6', $^3J_{CF}$ = 9.2 Hz), 130.39 (*s*), 133.64 (*s*), 134.47 (*s*), 145.43 (*s*), 150.51 (*s*), 156.21 (*s*), 156.45 (*s*), 157.24 (*s*), 158.21 (*s*), 163.84 (*d*, C-4', $^1J_{CF}$ = 256.2 Hz). MS, *m/z* (I_{rel} (%)): 392 [M]$^+$ (47), 239 [M–chloroisobenzoxazole]$^+$ (100), 118 [M–chloroisobenzoxazole-FC$_6$H$_4$CN]$^+$ (27). Found, %: C 64.34, H 3.70, N 14.19. $C_{21}H_{14}ClFN_4O$. Calculated, %: C 64.21, H 3.59, N 14.26.

2.4. Molecular docking studies

Protein preparation. The ligand protein complex CK2 with the azolopyrimidine derivative CHEMBL2062585 (PDB ID: 3U4U) was uploaded from the Protein Data Bank database in .pdb format. Further, in the ArgusLab 4.0.1 software, third-party molecules (water, ions, etc.) were removed from the complex and then hydrogen atoms were added. Binding site was determined relative to the position of native ligand with nanomolar activity (IC_{50} = 3 nM). Validation of docking parameters was carried out by redocking the native ligand with the following parameters: GADock (elitism: 3), Scoring function: Ascore, Binding site box size: 18.6×17.5×16.5 Å, Grid resolution: 0.2 Å.

A quantitative assessment of the docking protocol was carried out according to the RMSD (root-mean-square deviation). For the native structure RMSD < 2 Å, which indicates sufficient calculation accuracy. The parameters used for redocking were then used for docking the studied structures without changes.

Ligand preparation. Ligands were prepared in DataWarrior software. 3D coordinates of the ligands (1 conformer per 1 structure) were generated using the Self-organized algorithm and the MMFF94s+ force field.

Docking protocol. Molecular docking was performed in ArgusLab 4.0.1 software on a previously prepared protein with established parameters and binding site size. For docking, the Lamarckian genetic algorithm GADock and the empirical function AScore were used to calculate the free binding energy; the protein is taken as a rigid structure, and the ligands are flexible. A quantitative assessment of the affinity of ligands to the protein was carried out by analyzing the calculated docking score.

For the hit compound **9a** with the best (lowest) docking score, refined docking (Grid resolution 0.1 Å) was carried out with the initial generation of structures in ArgusLab with geometry optimization on the UFF molecular force field. The evaluation of docking results, i.e., the calculation of the 3D position of the hit compound in the target protein and the 2D-map of non-covalent interactions, was carried out in ArgusLab and the PoseView module of the proteins.plus web service, respectively.

2.5. CK2 Assay

Kinase activity was determined using the CK2a1 enzyme system (Promega V4482, Madison, WI, USA) and the ADP-GloTM kit (Promega V9101, Madison, USA) in white 96-well plates (Nunc U96 Microwell 267350, Denmark). Bovine casein was used as the peptide substrate. Staurosporine ATP-competitive inhibitor (STS, CAS 62996-74-1, Alfa Aesar J62837, 99 +%) was used as a positive control. The assay was carried out using 10 ng/well of N-GST labelled human recombinant CK2a1 expressed in Sf9 cells, 0.1 mg/mL casein, 10 mM ATP in a 40 mM Tris buffer (pH 7.50) containing 20 mM $MgCl_2$, 0.1 mg/mL BSA and 50 mM DTT. Compounds were introduced in 1.25% DMSO and

 DOI: 10.15826/chimtech.2023.10.2.11

preincubated with kinase at 450 rpm for 10 min. The reaction was carried out for 60 min at 25 °C in PST-60HL shaker (Biosan, Latvia). ATP-dependent luminescence was measured at an integration time of 1000 ms using Infinite M200 PRO microplate reader (Tecan GmbH, Grödig, Austria). The experiments were run in two replicates. The activity of CK2 in the sample wells was normalized against the control and enzyme-blank wells.

2.6. MTT assay and cell culture

MDA-MB-231 breast cancer cells and WI-26 VA4 lung epithelial-like cells were purchased from the ATCC (Manassas, VA, USA). MDA-MB-231 cells were maintained in Dulbecco's modified Eagle's medium (DMEM), supplemented with 1× non-essential amino acids, 25 mM Hepes, 1× penicillin/streptomycin, and, where indicated, 10% (v/v) foetal bovine serum (FBS), all obtained through Gibco (Thermo Fisher Scientific, Inc., Waltham, MA, USA) [37]. WI-26 VA4 cells were maintained in Advanced MEM (Gibco, Loughborough, UK) supplemented with 5% fetal bovine serum (Fetal Bovine Serum, qualified, Australia, Gibco, UK), penicillin (100 UI mL^{-1}), streptomycin (100 mg mL^{-1}), and GlutaMax (1.87 mM, Gibco, Loughborough, UK). All all cell lines were cultivated under a humidified atmosphere of 95% air/5% CO_2 at 37 °C. Subconfluent monolayers, in the log growth phase, were harvested by a brief treatment with TrypLE Express solution (Gibco, Loughborough, UK) in phosphate buffered saline (PBS, Capricorn Scientific, Germany) and washed three times in serum-free PBS. The number of viable cells was determined by trypan blue exclusion.

The effects of the synthesized compounds on cell viability were determined using the MTT colorimetric test [38]. All examined cells were diluted with the growth medium to $3.5 \cdot 10^4$ cells per mL, and the aliquots ($7 \cdot 10^3$ cells per 200 mL) were placed in individual wells in 96-well plates (Eppendorf, Hamburg, Germany) and incubated for 24 h. The next day, the cells were treated with the synthesized compounds separately in 10 and 100 mM concentrations (or 200.0 mM concentration and diluted at various concentrations for determination of IC50) and incubated for 72 h at 37 °C in 5% CO_2 atmosphere. Each compound was tested in triplicate. After incubation, the cells were treated with 40 mL MTT solution (3-(4,5-dimethylthiazol-2-yl)-2,5-diphenyltetrazolium bromide, 5 mg mL^{-1} in PBS) and incubated for 4 h. After additional 4 h incubation, the medium with MTT was removed and DMSO (150 mL) was added to dissolve the formazan crystals. The plates were shaken for 10 min. The optical density of each well was determined at 560 nm using GloMax Multi+ (Promega, Madison, WI, USA) microplate reader. Each of the tested compounds was evaluated for cytotoxicity in three separate experiments. All stock solutions for biological evaluations were prepared via dissolving synthesized compounds in DMSO.

3. Results and Discussion

3.1. Synthesis

Synthesis of hydrazones **3c,d** was realized by the heating of 2-phenyl-4-hydrazino-6,7-difluoroquinazoline **4a** [24], with 3,5-di(*t*-butyl)-2-hydroxybenzaldehyde and 5-chloro-2-hydroxybenzaldehyde, respectively (Scheme 1).

For obtaining 2-(4-fluorophenyl)-derivatives **9a**,**b** we performed the synthesis of 4-hydrazinoquinazoline **4b**. The key intermediate **7** was synthesized by condensation of 2-aminobenzamide **5** with 4-fluorobenzaldehyde (under stirring in ethanol at room temperature) and subsequent oxidation of azomethine **6** with copper(II) chloride (Scheme 2). Earlier, the synthesis of 2-(4-fluorophenyl)quinazolin-4-one **7** from aminoamide **5** and 4-fluorobenzaldehyde was achieved in the presence of other oxidants, such as iodine in ionic liquid [$bmim^+$][BF_4^-] [25], antimony chloride without solvent at microwave irradiation [26], or air in the presence of vanadium bis(acetylacetonate) $VO(acac)_2$ as a catalyst [27]. The formation of intermediate **6** in [$bmim^+$][BF_4^-] at room temperature was mentioned [25]. Notably, that interaction between anthranilamide **5** and aryl carbaldehydes leads to the formation of Schiff bases or 2,3-dihydroquinazolin-4(1*H*)-ones depending on the reaction conditions and the nature of aldehydes [28]. Therefore, it is not surprising that at room temperature the interaction of 4-fluorobenzaldehyde and aminoamide **5** resulted in the formation of azomethine **6**. The chloro-derivative **8** obtained by refluxing of quinazolinone **7** with phosphorus oxychloride was used for the introduction of the hydrazine group into position 4. The synthesis of hydrazones **9a**,**b** was carried out by heating of 2-(4-fluorophenyl)-4-hydrazinoquinazoline **4b** with correspondent aldehyde in ethanol (Scheme 2).

The structure of target quinazolines **3c**, **d** and **9a**,**b** was determined based on their ^{1}H NMR, ^{19}F NMR and ^{13}C NMR spectroscopy as well as mass spectrometry data (Figures S1-S18).

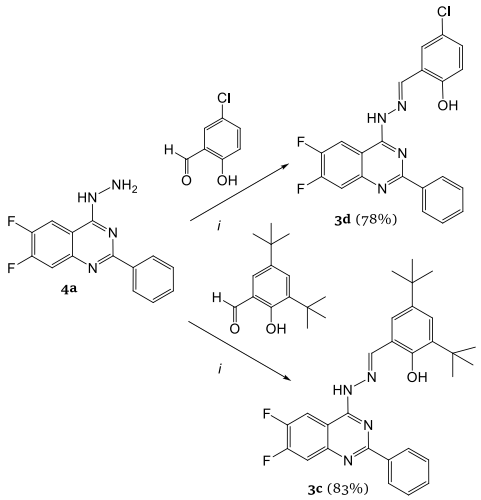

Scheme 1 Synthesis of 2-phenyl-6,7-difluoro-4-salicylidenehydrazino quinazolines **3c,d**. Reaction conditions: (*i*) ethanol, reflux, 1.5 h.

 DOI: 10.15826/chimtech.2023.10.2.11

The ^{1}H NMR spectra of salicylidenehydrazones **3c**,**d**, **9a**,**b** (Figures S1, S5, S11, S15) characteristically showed signals of aryl fragment protons, benzene or difluorobenzene ring, singlets of –CH=N-groups at 8.57–8.70 ppm, broaden singlets of NH at 12.0–12.2 ppm and OH at 12.0–13.3 ppm. Two doublet signals present at ^{19}F{H} NMR spectra of compounds **3c**,**d**, and one singlet in the case of derivatives **9a**,**b**. Structures **3c**,**d** and **9a**,**b** are also evidenced by the mass spectra data; the relative intensities of molecular ion peaks are 47–99%. The most abundant ions in the mass spectra of the correspondent 2-aryl-4-aminoquinazolines are m/z 257 for 2-phenyl-6,7-difluoroquinazolines **3c**,**d** and m/z 239 for 2-(4-fluorophenyl)quinazolines **9a**,**b**, which can form due to isobenzoxazole elimination.

3.2. Molecular docking

Molecular docking was performed using ArgusLab 4.0.1 software [29]. Previously, a protein-ligand complex was taken from the Protein Data Bank database [30]: a CK2 complex with the azolopyrimidine derivative CHEMBL2062585 [31] (PDB ID: 3U4U) [32]. After preparation (see Experimental) validation of the docking protocol was carried out for the protein-ligand complex by redocking the native ligand as a nanomolar inhibitor. According to the results of redocking, the standard deviation (RMSD) of the known position of CK2 protein inhibitor was 1.5 Å (Figure S19).

The results of molecular docking of several studied ligands prepared in DataWarrior [33] (see Experimental) with the calculated free binding energy (ΔG) as individual activity indicator are given in Table 1. All docking compounds are more active than the comparison compound CHEMBL2062585 (IC_{50} (CK2) = 3 nM).

To deepen the understanding of the action mechanism of probable CK2 inhibitors among the studied quinazoline derivatives, an updated docking refinement was carried out for the leader compound **9a** based on *in silico* activity indicators. The position of the calculated ligand **9a** in the active site of the protein with the recalculated values of Δ*G* is presented in Figure S20A. The profile of non-covalent interactions is defined using the PoseView module of the proteins.plus service [34, 35].

Molecular docking towards CK2 shows higher *in silico* activity with partial coincidence of non-covalent interactions for all compounds compared to known nanomolar inhibitor of this protein. *In silico* experiment revealed two hit compounds with the best affinity for casein kinase 2: the Δ*G* value for hydrazone **3a** is –13.91 kcal/mol, and for derivative **9a** Δ*G* = –14.16 kcal/mol (Table 1).

The leader compound **9a** is characterized by another binding method to the CK2 active site compared to the native ligand (Figure S20B). The main contribution to the binding of **9a** with the protein is made by several hydrophobic interactions (Figures 2, S20C), π-π stacking between the fluorophenyl moiety and the residue Phe113, and a hydrogen bond between the hydroxy group of the ligand and the residue His160. At the same time, both native ligand and **9a** are characterized by interactions only with residues of Asp175 and Met163.

Thus, despite the significant *in silico* activity of **9a** in terms of free binding energy relative to the nanomolar CK2 inhibitor, a different profile of non-covalent interactions can influence negatively the *in vitro* experiments.

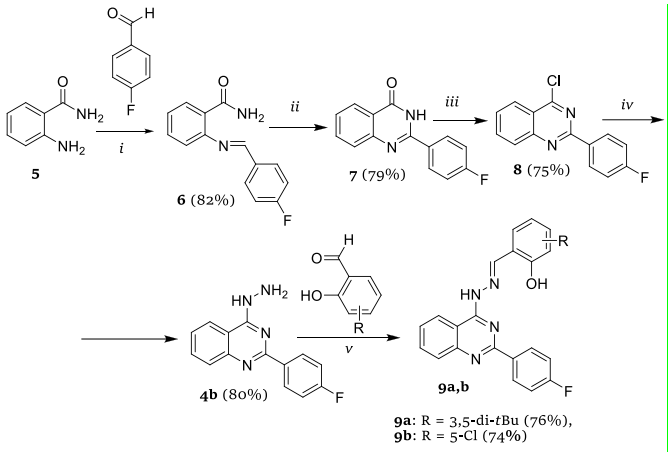

Scheme 2 Synthesis of 2-(4-fluorophenyl)-4-salicylidenehydrazino quinazolines **9a**,**b**. Reagents and conditions: (*i*) ethanol, r.t., 3 h; (*ii*) $CuCl_2$, ethanol, reflux, 5 h; (*iii*) $POCl_3$, reflux, 2 h, (*iv*) H_2N-NH_2·H_2O, ethanol, 70 °C, 3 h; (*v*) ethanol, reflux, 1.5 h.

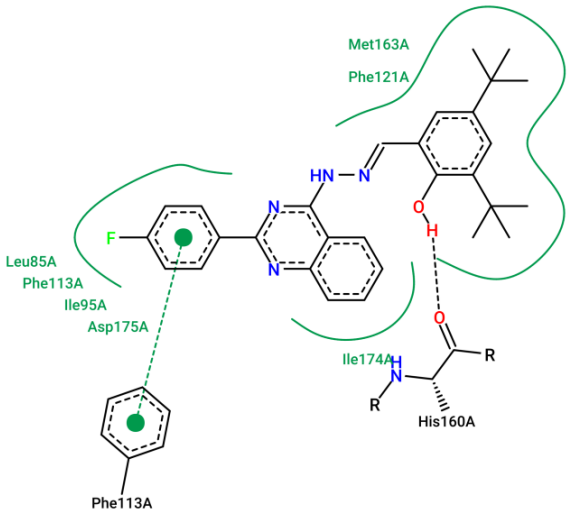

Figure 2 Non-covalent interactions of the docked ligand **9a**.

Table 1 Docking results and indicators of *in vitro*/*in silico* activity to casein kinase 2.

Compound	Δ*G*, kcal/mol	Compound	Δ*G*, kcal/mol
1a	–12.33	**3a**	–13.91
1b	–13.16	**3b**	–12.47
1c	–12.20	**3c**	–11.33
2a	–11.84	**3d**	–12.69
2b	–12.77	**9a**	–14.16 –13.86*
2c	–13.10	**9b**	–12.70
CHEMBL 2062585 (IC_{50} = 3 nM)	–10.67		

* The docking score obtained after docking refinement

 DOI: 10.15826/chimtech.2023.10.2.11

3.3. CK2 inhibition and cytotoxicity study

The target compounds were evaluated against human recombinant CK2 using the luminescent ADP-GloTM assay. Due to the limited solubility of the compounds, only four derivatives **1a**, **3c**, **9a**,**b** was tested. The CK2 activity was determined after the casein phosphorylation reaction by the value of ATP-dependent luminescence. The data obtained and the CK2 activity in the presence of 50 μM of the tested compounds are shown in Table 2. Initial screening at 50 μM revealed that the compounds are not active towards CK2.

All tested compounds showed no inhibitory activity at the level of the reference drug (Table 2). Even though the compounds **1**, **3**, **9** did not act as inhibitors of casein kinase 2, their cytostatic activity was investigated, since a different mechanism of cytotoxic action is possible.

Some hydrazonoquinazolines **1**, **3**, **9** were evaluated for their anticancer properties against MDA-MB-231 cells. Additionally, non-cancerous lung fibroblast cells WI-26 VA4 were used to control non-specific cytotoxicity (Table 3, Figure S21).

As can be concluded from the Table 3, compounds **1b**, **3b–d** and **9b** possess pronounced antiproliferative activities against MDA-MB-231 cells with IC_{50} values ranging between 4.91 and 65.2 μM. Noteworthy, non-cancerous lung fibroblast WI-26 VA4 cell line was less sensitive only to two tested molecules, including the most active nitrosalicylidene derivative **3b**.

4. Limitations

Structural modification is required to improve the solubility and bioavailability of the compounds. Unfortunately, the possibilities of purchasing reagents for various modifications are limited, and study of expanded range of compounds is hardly achievable.

5. Conclusions

The novel fluorine-containing 2-aryl-4-salicilidenhydrazino quinazolines **3, 9** were synthesized and characterized by using NMR and MS, and all the data are in accordance with the proposed structures. The results of molecular docking clearly indicate a high potential activity of this series of compounds in terms of free binding energy. On the other hand, other profiles of non-covalent interactions of the leader compounds compared to the nanomolar inhibitor can have various consequences. Therefore, an *in vitro* activity study with an *in vitro-in silico* correlation assay is expected to be the best direction for further targeted development of CK2 inhibitors for the considered class of compounds. N-(6,7-Difluoro-2-phenylquinazolin-4-yl)-N'-(5-nitrosalicylidene)hydrazine **3b** exhibited enhanced activity against breast cancer (MDA-MB-231) cells in combination with moderate selectivity toward normal WI-26 VA4 cells. The rest of compounds do not show noticeable selectivity to normal and tumour cells.

• Supplementary materials

This manuscript contains supplementary materials, which are available on the corresponding online page.

• Funding

This work was supported by the Ministry of Science and Higher Education of the Russian Federation, State Contract no FEUZ-2023-0021 (N687.42B.325/23).

• Acknowledgments

Authors thank Academician Alexander A. Spasov (Department of Pharmacology & Bioinformatics, Scientific Center for Innovative Drugs, Volgograd State Medical University) for assistance with study of human recombinant CK2 inhibition and the Head of Medicinal Chemistry Center Alexander S. Bunev (Togliatti State University) for cytotoxicity data.

• Author contributions

Conceptualization: E.V.N., S.K.K.
Data curation: E.V.N.
Investigation: M.D.L.
Methodology: E.V.N, M.D.L., I.I.B.
Software: I.I.B.
Validation: I.I.B.
Visualization: I.I.B.
Writing – original draft: E.V.N.
Writing – review & editing: S.K.K.
Project administration: S.K.K.

Table 2 Data of CK2 inhibition activity study for some hydrazonoquinazolines.

Compound	CK2 Activity (m±SD), %	CK2 Inhibition at 50 μM (m±SD), %
1a	102.14±18.22	−2.14±18.22
3c	94.5±14.98	5.5±14.98
9a	96.02±22.88	3.98±22.88
9b	108.16±1.1	−8.16±1.1
Staurosporine	7.87±1.34*	92.13±1.34*

Statistical significance relative to negative control, 1-factor ANOVA; *p <0.05

Table 3 MTT assay results for 2-aryl-4-salicylidenehydrazino quinazolines against breast cancer cell line (MDA-MB-231).

Compound	IC_{50}, μM	
	MDA-MB-231 (Breast cancer)	**WI26 VA4 (Normal cell)**
1a	>100	46.6±12.57
1b	65.2±7.67	69.81±9.15
3b	**4.91±0.66**	**6.32±0.47**
3c	41.9±12.6	17.49±2.41
3d	7.43±0.87	4.02±0.38
9a	n.d.	42.4±4.75
9b	14.5±1.80	11.27±1.02

n.d. – no data

 DOI: 10.15826/chimtech.2023.10.2.11

• Conflict of interest

The authors declare no conflict of interest.

• Additional information

Author IDs:

Emiliya V. Nosova, Scopus ID 35498195300;
Margarita D. Likhacheva, Scopus ID 58084945000;
Svetlana K. Kotovskaya, Scopus ID 6602187240;
Ilya I. Butorin, Scopus ID 57202983112.

Websites:

Ural Federal University, https://urfu.ru/en;
I. Postovsky Institute of Organic Synthesis, https://iosuran.ru.

References

1. Furman RR, Sharman JP, Coutre SE, Cheson BD, Pagel JM, Hillmen P, Barrientos JC, Zelenetz AD, Kipps TJ, Flinn I, Ghia P, Eradat H. Resistance mechanisms for the Bruton's tyrosine kinase inhibitor ibrutinib. N Engl J Med. 2014;370(24):997–1007. doi:10.1056/NEJMoa1400029
2. Chen X, Li W, Hu X, Geng Y, Wang R, Yin Y, Shu Y. Biomed Pharmacother. 2011;65(8):542–546. doi:10.1016/j.biopha.2011.04.017
3. Laramas M, Pasquier D, Filhol O, Ringeisen F, Descotes JL. Nuclear localization of protein kinase CK2 catalytic subunit (CK2α) is associated with poor prognostic factors in human prostate cancer. Eur J Cancer. 2007;43(5):928–934. doi:10.1016/j.ejca.2006.11.021
4. Charoenrat P, Rusch V, Talbot SG, Sarkaria I, Viale A, Socci N, Ngai I, Rao P, Singh B. Casein kinase II alpha subunit and C1-inhibitor are independent predictors of outcome in patients with squamous cell carcinoma of the lung. Clin Cancer Res. 2004;10(17):5792–5803. doi:10.1158/1078-0432.CCR-03-0317
5. Ortega CE, Seidner Y, Dominguez I. Mining CK2 in Cancer. PLoS ONE 2014;9(12):e115609. doi:10.1371/journal.pone.0115609
6. Faust RA, Gapany M, Tristani P, Davis A, Adams GL, Ahmed K. Elevated protein kinase CK2 activity in chromatin of head and neck tumors: association with malignant transformation. Cancer Lett. 1996;101(1):31–35. doi:10.1016/0304-3835(96)04110-9
7. Faust RA, Niehans G, Gapany M, Hoistad D, Knapp D, Cherwitz D, Davis A, Adams GL, Ahmed K. Subcellular immunolocalization of protein kinase CK2 in normal and carcinoma cells. Int J Biochem Cell Biol. 1999;31(9):941–949. doi:10.1016/s1357-2725(99)00050-3
8. Gapany M, Faust RA, Tawfic S, Davis A, Adams GL, Ahmed K. Association of elevated protein kinase CK2 activity with aggressive behavior of squamous cell carcinoma of the head and neck. Mol Med. 1995;1(6):659–666.
9. Kim HS, Chang YG, Bae HJ, Eun JW, Shen Q, Park SJ, Shin WC, Lee EK, Park S, Ahn YM, Park WS, Lee JY, Nam SW. Oncogenic potential of CK2α and its regulatory role in EGF-induced HDAC2 expression in human liver cancer. FEBS J. 2014;281(3):851–861. doi:10.1111/febs.12652
10. Rabjerg M, Bjerregaard H, Halekoh U, Jensen BL, Walter S, Marcussen N. Molecular characterization of clear cell renal cell carcinoma identifies CSNK2A1, SPP1 and DEFB1 as promising novel prognostic markers. APMIS. 2016;124(5):372–383. doi:10.1111/apm.12519
11. Nitta RT, Gholamin S, Feroze AH, Agarwal M, Cheshier SH, Mitra SS, Li G. Casein kinase 2α regulates glioblastoma brain tumor-initiating cell growth through the β-Catenin pathway. Oncogene. 2014;34(28):3688–3699. doi:10.1038/onc.2014.299
12. Pagano MA, Cesaro L, Meggio F, Pinna LA. Protein kinase CK2: a newcomer in the 'Druggable Kinome'. Biochem Soc Trans. 2006;34(6):1303–1306. doi:10.1042/BST0341303
13. Guerra B, Issinger O-G. Protein kinase CK2 in human diseases. Curr Med Chem. 2008;15(19):1870–1886. doi:10.2174/092986708785132933
14. Silva-Pavez E, Tapia J. Protein kinase CK2 in cancer energetics. Front Oncol. 2020;10:893. doi:10.3389/fonc.2020.00893
15. Borgo C, D'Amore C, Sarno S, Salvi M, Ruzzene M. Protein kinase CK2: a potential therapeutic target for diverse human diseases. Curr Signal Transduct Ther. 2021;6(1):1–20. doi:10.1038/s41392-021-00567-7
16. Chua MMJ, Lee M, Dominguez I. Cancer-type dependent expression of CK2 transcripts. PLoS ONE. 2017;12(12):e0188854. doi:10.1371/journal.pone.0188854
17. Haddach M, Pierre F, Regan CF, Borsan C, Michaux J, Stefan E, Kerdoncuff P, Schwaebe MK, Chua PC, Siddiqui-Jain A, Macalino D, Drygin D, O'Brien SE, Rice WG, Ryckman DM. Synthesis and SAR of inhibitors of protein kinase CK2: novel tricyclic quinoline analogs. Bioorg Med Chem Lett. 2012;22(1):45–48. doi:10.1016/j.bmcl.2011.11.087
18. Lyapustin DN, Kotovskaya SK, Butorin II, Ulomsky EN, Rusinov VL, Babkov DA, Pokhlebin AA, Spasov AA, Melekhin VV, Tokhtueva MD, Shcheglova AV, Makeev OG. CK2 inhibition and antitumor activity of 4,7-Dihydro-6- nitroazolo[1,5-a]pyrimidines. Mol. 2022;27(16):5239. doi:10.3390/molecules27165239
19. Iegre J, Atkinson EL, Brear PD, Cooper BM, Hyvönen M, Spring DR. Chemical probes targeting the kinase CK2: a journey outside the catalytic box. Org Biomol Chem. 2021;19(20):4380–4396. doi:10.1039/d1ob00257k
20. Dowling JE, Alimzhanov M, Bao L, Chuaqui C, Denz CR, Jenkins E, Larsen NA, Lyne PD, Pontz T, Ye Q, Holdgate GA, Snow L, O'Connell N, Ferguson AD. Potent and Selective CK2 Kinase inhibitors with effects on Wnt pathway signaling in vivo. ACS Med Chem Lett. 2016;7(3):300–305. doi:10.1021/acsmedchemlett.5b00452
21. Wells CI, Drewry DH, Pickett JE, Tjaden A, Krämer A, Müller S, Gyenis L, Menyhart D, Litchfield DW, Knapp S, Axtman AD. Development of a potent and selective chemical probe for the pleiotropic kinase CK2. Cell Chem Biol. 2021;28(4):546–558. doi:10.1016/j.chembiol.2020.12.013
22. Dalle Vedove A, Zonta F, Zanforlin E, Demitri N, Ribaudo G, Cazzanelli G, Ongaro A, Sarno S, Zagotto G, Battistutta R, Ruzzene M, Lolli G. A novel class of selective CK2 inhibitors targeting its open hinge conformation. Eur J Med Chem. 2020;195:112267. doi:10.1016/j.ejmech.2020.112267
23. Oshima T, Niwa Y, Kuwata K, Srivastava A, Hyoda T, Tsuchiya Y, Kumagai M, Tsuyuguchi M, Tamaru T, Sugiyama A, Ono N, Zolboot N, Aikawa Y, Oishi S, Nonami A, Arai F, Hagihara S, Yamaguchi J, Tama F, Kunisaki Y, Yagita K, Ikeda M, Kinoshita T, Kay SA, Itami K, Hirota T. Cell-based screen identifies a new potent and highly selective CK2 inhibitor for modulation of circadian rhythms and cancer cell growth. Sci Adv. 2019;5(1):9060–9083. doi:10.1126/sciadv.aau9060
24. Trashakhova TV, Nosova EV, Slepukhin PA, Valova MS, Lipunova GN, Charushin VN. 2-Hydroxybenzaldehyde (2-phenylquinazolin-4-yl)hydrazones and their ZnII complexes: synthesis and photophysical properties. Russ Chem Bull. 2011;60(11):2347–2353. doi:10.1007/s11172-011-0360-z
25. Wang X-S, Yang K, Zhang M-M, Yao C-S. Synthesis of 2-Arylquinazolin-4(3H)-one derivatives catalyzed by iodine in [bmim$^+$][BF_4^-]. Synth Commun. 2010;40(17):2633–2646. doi:10.1080/00397910903318609
26. Kang H, Wang W, Sun Q, Yang S, Jin J, Zhang X, Ren X, Zhang J, Zhou J. Microwave-assisted synthesis of quinazolin-4(3*H*)-ones catalyzed by $SbCl_3$. Heterocycl Commun. 2018;24(6):293–296. doi:10.1515/hc-2018-0115

 DOI: 10.15826/chimtech.2023.10.2.11

27. Zhan D, Li T, Zhang X, Dai C, Wei H, Zhang Y, Zeng Q. Vanadium-catalyzed synthesis of 4(3H)-quinazolinones from anthranilamides and aryl aldehydes. Synth Commun. 2013;43(18):2493–2500. doi:10.1080/00397911.2012.717669
28. Tímea M, Miklós F, Lázár L, Fülöp F. Synthesis of 2-(hetero)arylquinazolinones in aqueous media. Arkivoc. 2016;2016(vi):257–258. doi:10.24820/ark.5550190.p009.894
29. Thompson MA. Molecular docking using ArgusLab, an efficient shape-based search algorithm and the AScoring function. ACS meeting:Philadelphia; 2004. 42.
30. Berman HM, Westbrook J, Feng Z, Gilliland G, Bhat TN, Weissig H, Shindyalov IN, Bourne PE. The protein data bank. Nucleic Acids Res. 2000;28(1):235-242. doi:10.1093/nar/28.1.235
31. Somoza JR, Koditek D, Villaseñor AG, Novikov N, Wong MH, Liclican A, Xing W, Lagpacan L, Wang R, Schultz BE, Papalia GA, Samuel D, Lad L, McGrath ME. Structural, biochemical, and biophysical characterization of idelalisib binding to phosphoinositide 3-kinase δ. J Biol Chem. 2015;290(13):8439-8446. doi:10.1074/jbc.M114.634683
32. Gaulton A, Hersey A, Nowotka M, et al. The ChEMBL database in 2017. Nucleic Acids Res. 2017;45(D1):D945–D954. doi:10.1093/nar/gkw1074
33. Sander T, Freyss J, von Korff M, Rufener C. DataWarrior: an open-source program for chemistry aware data visualization and analysis. J Chem Inf Model. 2015;55(2):460–473. doi:10.1021/ci500588j
34. Schöning-Stierand K, Diedrich K, Fährrolfes R, Flachsenberg F, Meyder A, Nittinger E, Steinegger R, Rarey M. ProteinsPlus: interactive analysis of protein–ligand binding interfaces. Nucleic Acids Res. 2020;48(W1):W48–W53. doi:10.1093/nar/gkaa235
35. Stierand K, Maass PC, Rarey M. Molecular complexes at a glance: automated generation of two-dimensional complex diagrams. Bioinform. 2006;22(14):1710–1716. doi:10.1093/bioinformatics/btl150
36. Karasala BK, Gollamudi P, Inkollu B, Vidavalur S. Russ J Org Chem. 2020;56(8):1446–1454. doi:10.1134/S1070428020080163
37. Horgan CC, Nagelkerke A, Whittaker TE, Nele V, Massi L, Kauscher U, Penders J, Bergholt MS, Hood SR, Stevens MM. Molecular imaging of extracellular vesicles *in vitro* via Raman metabolic labelling. J Mater Chem B. 2020;8(20):4447–4459. doi:10.1039/D0TB00620C
38. Sylvester PW. Optimization of the tetrazolium dye (MTT) colorimetric assay for cellular growth and viability. Methods Mol Biol. 2011;716:157–168. doi:10.1007/978-1-61779-012-6_9

 DOI: 10.15826/chimtech.2023.10.2.11